Statistical-Mechanical Model of Protein Precipitation by Nonionic Polymer

A theoretical approach to predict the solubility of proteins in solutions containing nonionic polymer is presented. The effective protein-protein interaction due to the presence of the polymer is related to the volume-exclusion potential of Asakura and Oosawa. Statistical-mechanical perturbation theory, as originally applied by Gast et al. to model colloidal flocculation, is used to calculate free energies, from which solubility curves for varying protein-polymer diameter ratios are obtained. The theory correctly predicts all the trends observed in experimental studies of these systems. To explain the influence of process parameters such as the pH and the ionic strength on protein solubility, the intermolecular potential is improved by the addition of an electrostatic interaction term. It is found that the theoretical predictions of the variation in protein solubility, both with the solution pH and the ionic strength, are in accordance with experimental observations.

Hari Mahadevan
Carol K. Hall
Department of Chemical Engineering
North Carolina State University
Raleigh, NC 27695

Introduction

The rapid development of the biotechnology industry in the last decade has accelerated the demand for not only more but also purer forms of proteins and enzymes. This demand stems from a variety of industries including the food, alcoholic beverages, paper, pharmaceutical and textile industries and from the medical profession (Faith et al., 1971). The list of commercial and medical applications for proteins is long and is expected to grow as genetic engineering technology advances. To maximize the benefits from these advances, it is important to strengthen efforts to modify and improve protein separation and recovery processes.

Two key considerations in the selection of a bioseparations and recovery process are that it be relatively gentle and easily adaptable to large-scale production. The reason for the first requirement is that proteins are very sensitive to any changes in their environment. The unique structure-function relationship of these biomolecules leads to denaturation if their environment is changed in a rapid and/or drastic manner. One of many separation techniques fulfilling the requirements noted above is fractional precipitation using polyethylene glycol (PEG). PEG is known not to denature proteins [even though some recent evidence appears to question this assertion (Lee and Lee, 1987)]. This technique also appears to be easily conducted on a large scale.

Protein precipitation is accomplished by causing either a protein or part of a mixture of proteins in solution to precipitate by altering a key property of the solvent. The precipitate can then be filtered out or recovered by centrifugation. In spite of the fact that protein precipitation is an important industrial and laboratory fractionation method, it is rather poorly understood at the fundamental level (Foster et al., 1973). The observed effects on the solubility resulting from changes in any of the process variables (pH, ionic strength and protein or polymer molecular weights) have yet to be explained or predicted completely.

Precipitation of proteins by nonionic polymers is a relatively well-established technique. High molecular weight polymers such as PEG have been used both in the laboratory and in pilot plants to precipitate proteins (Bjurstrom, 1985). One of the principal advantages of this technique is that the operation can be carried out at ambient temperatures since the polymer does not significantly interact with the protein. Comparatively low concentrations of polymer, on the order of 5–20 wt. %, are required to precipitate most proteins. The main hindrance to the large-scale use of this process is the difficulty of recycling the polymer. The polymer has proven to be hard to recover from the precipitated protein fraction (Bjurstrom, 1985; Scopes, 1982). However, it has been found that using PEG of a higher average molecular weight significantly reduces the contamination of the

Correspondence concerning this paper should be addressed to C. K. Hall.

precipitate with polymer (Knoll and Hermans, 1983). Knoll and Hermans presume that the size of the solvent interstices between the protein molecules in the precipitate phase is insufficient to accommodate larger polymer molecules. Hence, it might be appropriate to imagine that polymer molecules of average dimension as small as a protein molecule, or smaller, would partition measurably between the two phases, while larger polymer molecules would be excluded from the precipitate.

The solubility of single proteins and protein mixtures in solutions containing PEG has been studied extensively in recent years (Polson et al., 1964; Kula et al., 1965; Chun et al., 1967; Hönig and Kula, 1976; Bell et al., 1983). Atha and Ingham (1981), Ingham and coworkers (1977, 1978), Kula and coworkers (1965), Middaugh and coworkers (1978), Hasko (1982), and Haire and coworkers (1984) have measured precipitation curves, apparent solubilities and thermodynamic properties of various proteins in the presence of PEG under a variety of experimental techniques. Most studies have generated precipitation curves that relate protein solubility to PEG concentration. Knoll and Hermans (1983) used light scattering measurements to calculate thermodynamic interaction parameters for solutions containing bovine serum albumin (BSA) and PEG. A significant result of these studies is that different research groups using varying methods to study the mechanism of precipitation of proteins by PEG reached the conclusion that specific chemical interactions between protein and polymer were *absent*. The import of this finding is that, in the absence of any specific protein-polymer interaction, the primary mechanism for the phase separation is one of volume exclusion (also called steric hindrance or displacement).

The experiments conducted on protein-PEG solutions provide information on the thermodynamic properties of proteins in the absence of PEG as well as the incremental effect that PEG has on the thermodynamics of proteins. The apparent linearity of the logarithm of the protein solubility data over a wide range of PEG concentrations has been used by some authors to extract the apparent (intrinsic) solubility of protein in the absence of PEG thus allowing the determination of protein activities (Haire et al., 1984). We show later in this paper that the extraction of the intrinsic solubility in this manner may be incorrect as the linearity of the solubility curve does not extend to zero polymer concentration.

Four experimental trends have been observed in these studies:

1. Larger proteins tend to precipitate at lower PEG concentrations than do smaller ones, as shown in Figure 1.

2. At a fixed PEG concentration, the solubility of proteins increases with decreasing average molecular weight of PEG as shown in Figure 2. The slopes of these curves decrease with the molecular weight of the polymer, leveling off at a weight of about 10,000–20,000. Figures 1 and 2 are taken from the study of PEG-induced precipitation by Atha and Ingham (1981).

3. In the range within which experimental data has been taken, a semilogarithmic plot of solubility (in g/L) vs. concentration of PEG in w/v units (usually g/100 mL) is linear as seen in Figures 1 and 2.

4. The solubility decreases as the pH approaches the isoelectric point or as the ionic strength is increased

Most of the theories of polymer-induced protein phase separation are based on the thermodynamic theories of Ogston and coworkers (Ogston and Phelps, 1961; Ogston, 1962; Edmond and Ogston, 1968). Central to this approach is the idea that

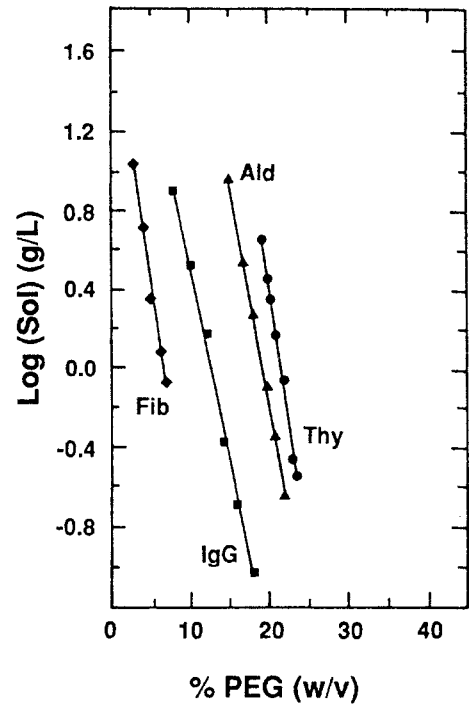

Figure 1. Solubility of various proteins in PEG-4000.
From D. H. Atha and K. C. Ingham, *J. Biol. Chem.*, **256**, 12108 (1981). See reference for details of solution conditions.

steric hindrance (or volume exclusion) is the primary mechanism by whch PEG induces phase separation in a protein solution. In other words, although the intrinsic solubility of a protein depends on pH, ionic strength, and other protein specific parameters, the addition of PEG to a protein solution decreases protein solubility by sterically excluding protein from regions of the solvent it normally occupies. Thus the protein is forced to concentrate until its solubility is exceeded and precipitation occurs (Knoll and Hermans, 1983; Haire et al., 1984; Laurent, 1963; Arakawa and Timasheff, 1985). However, earlier theories developed applying these arguments give results that agree with only a few of the experimental observations. For example, Atha

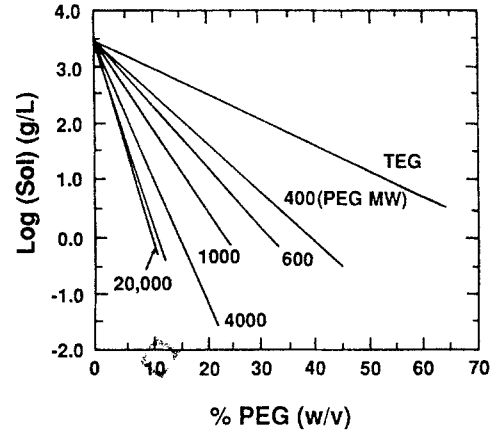

Figure 2. Effect of PEG molecular weight on solubility of human serum albumin.
From D. H. Atha and K. C. Ingham, *J. Biol. Chem.*, **256**, 12108 (1981). See reference for details of solution conditions.

and Ingham (1981) have analyzed the mechanism of protein precipitation by PEG in terms of excluded volume using the arguments described above. Their theory reproduces the correct trend for protein molecular weight and for the linearity of the solubility curve. However, they find that their predicted variation with polymer molecular weight is opposite to that observed experimentally, and they overestimate the dependence of the slopes of the solubility vs. polymer molecular weight curve. In addition, their theory does not address variations of the solubility with pH or ionic strength.

In this paper we apply a fundamental theory originally developed by Gast et al. (1983) to explain the precipitation of proteins using nonionic polymer. The objective of our work is to develop a comprehensive theory of protein solubility in the presence of a polymer. We employ this fundamental approach to predict the solubility of pure proteins in protein-polymer systems. The results for precipitation are presented in the form of solubility curves relating the logarithm of the solubility to the concentration of polymer added to the system. Also, alternate expressions for the solubility (independent of the protein diameter) are derived by relating its parametric variation with thermodynamic quantities such as the partial specific volume of the protein and its hydration.

The theory is developed by treating the precipitation as an equilibrium phase separation using standard techniques of statistical mechanics. The first step is the calculation of an effective protein-protein interaction potential (or potential of mean force) using models for protein-protein, protein-polymer and polymer-polymer interaction. Perturbation theory is then used to calculate chemical potentials and pressure for each phase. Next a thermodynamic stability analysis is employed to predict phase transformation, and thus a complete phase diagram is generated. Finally, the influence of the process parameters, such as polymer molecular weight, protein molecular weight, pH and ionic strength, on the phase diagram is studied. The predictions are compared with experimental data obtained from the literature. We find that the theory correctly predicts all four of the trends observed in experimental studies of these systems.

In the following two sections, we outline the theory and describe the statistical-mechanical analysis used to generate the phase diagrams, and then compare the results of the theoretically calculated solubilities with experimental data. Subsequently, the effect on the solubility of including electrostatic interactions between proteins is discussed.

Molecularly-Based Theory

In developing a fundamental theory to model the precipitation of proteins by nonionic polymer, we can draw on work done in the field of colloidal science. Described is the development of a theory grounded in statistical mechanics to model the phenomenon of protein precipitation. The theory is the same as that used by Gast et al. to model colloidal flocculation. For clarity, it is rederived.

Effective protein-protein interaction

A statistical-mechanical treatment of protein precipitation begins with a model for the interaction between molecules. Since we are treating the protein-polymer-solvent system as a pseudo-one-compartment system, we require a model for the effective interaction (or the potential of mean force) between protein molecules in the presence of polymer and solvent molecules.

First, we make the assumption that the effective protein-protein interaction potential is associated primarily with volume-exclusion effects and we ignore electrostatic effects. To calculate the effective interaction we model the protein molecules as hard spheres of diameter d_2 and the polymer molecules as spheres of diameter d_3 that cannot penetrate protein molecules but can penetrate each other. The solvent (species 1) is modeled as a continuous medium. Thus, surrounding each protein molecule is a shell of thickness $d_3/2$ which excludes all polymer molecules. Two protein molecules approaching closer than $2\,d_{23} = (d_2 + d_3)$ completely exclude polymer molecules from the region of overlap between their excluded shells. In the absence of the polymer, or when protein molecules are far enough apart, no attractive forces are felt among the protein molecules. However, when they are so close together that polymer cannot enter the void between the protein molecules, an unbalanced osmotic force due to the surrounding polymer and solvent molecules is created, tending to push the protein molecules together. This is called the volume-exclusion attraction, as illustrated in Figure 3.

The potential resulting from this attraction can be derived from geometric (projected area) considerations as was originally done by Asakura and Oosawa (1958) and later by deHek and Vrij (1981). It is also possible to derive the same potential from fundamental statistical mechanical roots as a potential of mean force between particles in a background fluid (Dickman, 1988). The resulting pair potential is:

$$U(r) = \begin{cases} \infty, & r < d_2 \\ -\dfrac{4}{3}\pi d_{23}^3 n_3 kT\left[1 - \dfrac{3r}{4d_{23}} + \dfrac{r^3}{16 d_{23}^3}\right], & d_2 \le r \le 2d_{23} \\ 0, & 2d_{23} < r \end{cases} \quad (1)$$

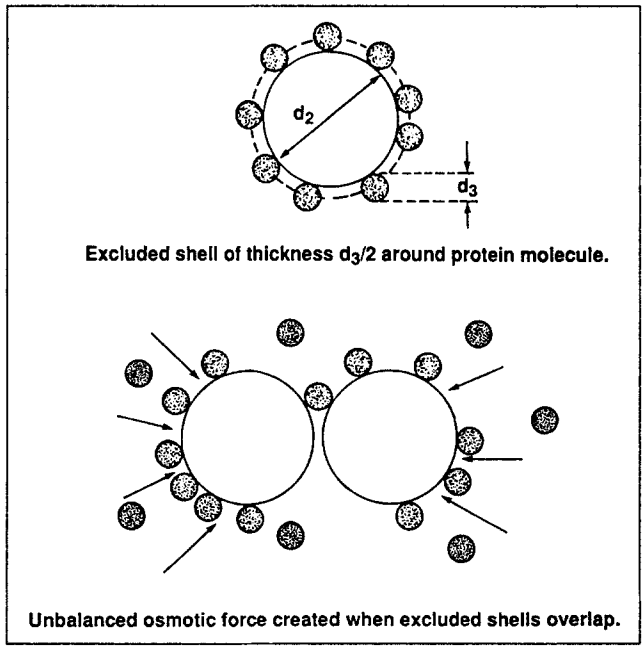

Figure 3. Volume-exclusion attraction between protein molecules due to the presence of the polymer.
Open circles are protein molecules, and filled circles are polymer molecules.

where r is the center-to-center separation, n_3 is the number density of polymer molecules in the polymer solution (discussed later), k is Boltzmann's constant, and T is the absolute temperature. Note that this equation assumes ideal conditions for the polymer consistent with our model. It is possible to treat nonidealities in the polymer-solvent interaction with, for instance, the inclusion of a second virial term in the expansion for the osmotic pressure (See Gast et al., 1983). However, this procedure involves an empiricism in the calculation of the second virial coefficient which we are anxious to avoid at this stage of the model development. Equation 1 describes the induced attraction between proteins due to volume exclusion of polymers by proteins. The depth of the attractive well increases with the diameter ratio of protein to polymer (d_2/d_3). The range of the protential, however, decreases as the diameter ratio is increased. Although this simple form for the interaction potential is somewhat unrealistic, it contains the essential physics of the problem. Also, it is easy to add contributions to the overall potential from other forces (e.g., electrostatic interactions), as deemed necessary by comparison with experimental data.

Perturbation theory

Perturbation theory is a method, based in statistical mechanics, for predicting the thermodynamic properties of a system. In this method, the pairwise interaction potential is decomposed into a reference potential and a perturbing potential. The reference potential describes a system with well-known thermodynamic properties; it is usually taken to be the hard-sphere potential $u_{hs}(r)$. The perturbing potential $u_p(r)$, is usually an attractive potential. The total pairwise interaction potential is the sum

$$U(r, \lambda) = u_{hs}(r) + \lambda\, u_p(r) \tag{2}$$

where λ, the perturbing parameter, may be used to vary the strength of the perturbation.

In perturbation theory, the logarithm of the configurational integral is expanded in a Taylor series about $\lambda = 0$. Perturbation theories differ in the type of expansions done about the perturbing parameter. Also, the order to which the expansions are carried out may vary, resulting in zero-, first- and second-order theories. Perturbation theory expansions are valid and remain numerically accurate as long as the $\mathcal{O}(\lambda^2)$ term is smaller than the $\mathcal{O}(\lambda)$ term, independent of the magnitude of λ itself. Gast et al. employed the perturbation expansion due to Barker and Henderson (1967). (In this case, since the volume-exclusion potential has a hard-core region, the effective hard-sphere diameter d, as defined by Barker and Henderson to annul two terms in their Taylor series, is not a function of temperature.)

The Helmholtz free energy, A, can be calculated directly from the perturbation expansion. The second-order perturbation expansion for the Helmholtz free energy as presented by Barker and Henderson, is

$$A/NkT = A_{hs}/NkT + \frac{\lambda\rho}{2}\int \frac{u_p(r)}{kT}\, g_{hs}(r)\, 4\pi r^2\, dr - \frac{\rho\lambda^2}{4}\left(\frac{\partial\rho}{\partial p}\right)_{hs} kT \int \left[\frac{u_p(r)}{kT}\right]^2 g_{hs}(r)\, 4\pi r^2\, dr + \mathcal{O}(\lambda^3) \tag{3}$$

where ρ is the density of protein molecules, p is the pressure, and g_{hs} and A_{hs} are the radial distribution function and the Helmholtz free energy of the hard-sphere reference state. In Eq. 3 we have used the macroscopic compressibility approximation to evaluate the second-order term.

Phase transition prediction requires knowledge of the Gibbs free energy, G, and the pressure, p, of the system of interest. These quantities can be calculated from the Helmholtz free energy as follows:

$$G/kT = \left.\frac{\partial(\rho A/kT)}{\partial\rho}\right|_T \tag{4}$$

$$p/kT = \rho G/kT - \rho A/kT \tag{5}$$

These thermodynamic properties can be calculated using a perturbation expansion provided there is an accurate expression for the requisite property of the reference system in the chosen state (phase). Very good approximations are available for the pressure, the Helmholtz and Gibbs free energies, and also for the radial distribution function of the hard-sphere system for both the fluid and solid phases. These equations are described below.

Equations of State for the Hard-Sphere Reference Systems. The free energies and the pressure for the hard-sphere reference system can be calculated from an equation of state expressing the compressibility factor, Z_{hs}, in terms of the volume fraction of the molecules. For the fluid phase, the Carnahan-Starling equation is used (Carnahan and Starling, 1970):

$$p_{hs}/\rho\, kT = Z_{hs} = \frac{1 + \phi_2 + \phi_2^2 - \phi_2^3}{(1 - \phi_2)^3} \tag{6}$$

where $\phi_2 = \rho\, d_2^3\pi/6$ is the volume fraction of the protein. For the solid phase, an equation of state developed by Hall (1971) as a Padé approximant to Monte Carlo data is used. The expression for Z_{hs} is in terms of β where $\beta = 4(1 - \phi_2/\phi_0)$, and ϕ_0 is the volume fraction at close packing. [$\phi_0 = (\pi/6)\sqrt{2}$ for a face-centered cubic lattice.]

$$Z_{hs} = 2.557696 + 0.1253077\beta + 0.1762393\beta^2 - 1.053308\beta^3 + 2.818621\beta^4 - 2.921934\beta^5 + 1.118413\beta^6 + [(12 - 3\beta)/\beta] \tag{7}$$

Radial Distribution Function for the Hard-Sphere Reference System. The radial distribution function for pairs of molecules is defined by:

$$g(r_{12}) = \frac{N!}{\rho^2(N-2)!} \times \frac{\int \cdots \int e^{-U_{TOT}/kT}\, dr_3 \cdots dr_N}{Z_N} \tag{8}$$

It is extremely difficult to calculate this quantity exactly even for hard spheres. There are, consequently, several approximate integral equations developed for the radial distribution functions of fluids. For the fluid phase, we use the explicit analytical solution to the Percus-Yevick equation developed by Smith and Henderson (1970) for the hard sphere $g(r)$ along with the Verlet-Weis correction (1972). For the solid-phase radial distribution function, we use the analytical approximation derived by

Kincaid and Weis (1977). Their expression is:

$$g_{hs}(r) = \frac{A}{r}\exp\left[-W_1^2(r-r_1)^2 - W_2^4(r-r_1)^4\right] + \frac{W}{24\phi\sqrt{\pi}} \times \sum_{i=2}^{\infty} \frac{n_i}{rr_i}\exp\left[-W^2(r-r_i)^2\right] \quad (9)$$

The expressions for the calculation of the r_i's and the parameters, A, ϕ, W, W_1, and W_2, are given in the publication by Kincaid and Weis (1977). Note that the series is terminated at $i = 5$ as suggested by Kincaid and Weis. Equation 9 is valid for a wide range of reduced densities ranging from 0.50 to arbitrarily near the close-packed value of 0.74.

Phase diagram generation

The Helmholtz and Gibbs free energies and the pressure of the system are calculated for different volume fractions of polymer added, for both the fluid and the solid phases by substituting the reference system properties described above into Eqs. 3–5. The integration in Eq. 3 is done numerically using Simpson's rule. To determine the phases in equilibrium at a particular polymer concentration, the Gibbs free energy is plotted vs. the pressure in both the fluid and solid regimes as shown in Figure 4. The protein volume fraction varies continuously along both the fluid and solid curves. The transition from fluid to the solid phase occurs at the intersection of the two curves as shown in this figure. Also, from the coexistence pressure and/or the coexistence Gibbs free energy, the volume fraction of the protein can be found. The average CPU time required to obtain the Gibbs free energy-pressure curve on a Mico VAX II computer in the fluid phase (20 protein volume fractions) is 275 seconds. In the solid phase, it takes 150 seconds for 45 protein volume fractions.

Repetition of these calculations for different polymer concentrations (volume fractions) leads to the generation of the phase diagram which indicates the onset of the phase transition as a function of protein and polymer volume fractions. The parameters that can be varied are the protein and polymer diameters (or molecular weights), the volume fraction of polymer added (concentration), and the volume fraction of the protein in the fluid phase. Calculation of the Gibbs free energy and the pressure of the system using Eqs. 4 and 5 is done numerically, and a phase plot is thus generated.

Results of the Model

Phase diagrams

The results are presented in the form of phase diagrams (Figure 5) which show the variation of the volume fraction of the protein, ϕ_2, in the coexisting phases, as a function of the volume fraction of added polymer, ϕ_3. The volume fraction of the protein is, by definition, the ratio of the volume occupied by the protein molecules to total volume of the system: $\phi_2 = (N_2\pi d_2^3)/(V_{tot}6)$. The volume fraction of the added polymer ϕ_3, however, is the ratio of volume occupied by the polymer molecules to the volume *available* for the polymer molecules to occupy, where the volume available to the polymer molecules is the total volume less that taken up by the proteins: $\phi_3 = (\pi n_3 d_3^3)/6$. Figure 5 is drawn for different protein-to-polymer diameter ratios ranging from 2.69 to 10.0 for comparison with experimental data (see Table 1). The fluid, solid and the two-phase regions are shown. Data for the molecular diameters of the proteins and PEG-4000 were obtained from Atha and Ingham (1981), who calculated the radii of the equivalent hydrodynamic spheres for the proteins from measurements of the diffusion coefficient D, using $r_{prot} = kT/6\pi\eta D$ where η is the viscosity of the medium. The radius of the equivalent sphere for the polymer was calculated therein using $r_{poly} = (3.10^7[\eta]\overline{M}_2)/(4\pi N_{Av}\nu)$ where ν is Simha's factor (2.5 for suspended spheres), and the intrinsic viscosity $[\eta]$ was calculated using $[\eta] = KM_2^a$. [See Atha and Ingham (1981) for the molecular weight dependence and values of a and K.]

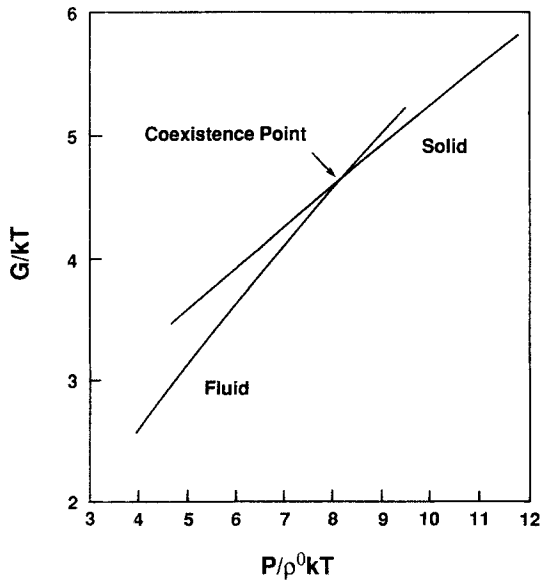

Figure 4. Thermodynamic stability analysis to determine the coexistence conditions.

ρ^o is the close-packed density.

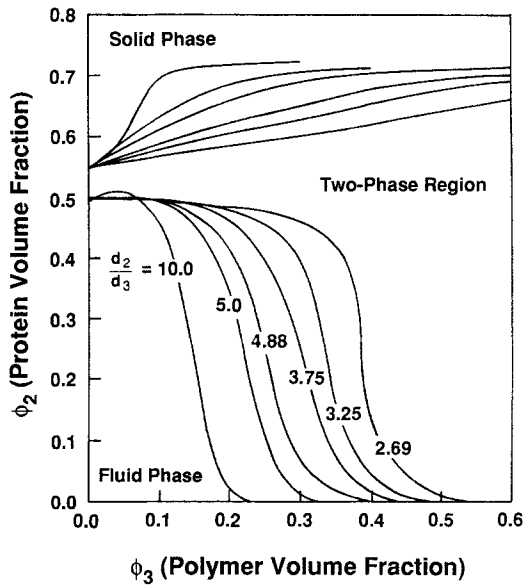

Figure 5. Phase diagram indicating compositions for various diameter ratios of protein to polymer.

Table 1. Diameter Ratios

Species	Diameter (cm)	System	d_2/d_3
Aldolase (ALD)	9.26×10^{-7}	ALD & PEG-4000	2.69
γ-Globulin (IgG)	11.18×10^{-7}	IgG & PEG-4000	3.25
Albumin (human serum)	7.04×10^{-7}	HSA & PEG-1000	3.75
Albumin (human serum)	7.04×10^{-7}	HSA & PEG-600	4.88
Thyroglobulin (THY)	17.22×10^{-7}	THY & PEG-4000	5.0
Albumin (human serum)	7.04×10^{-7}	HSA & PEG-400	5.86
Fibrinogen (FIB)	21.4×10^{-7}	FIB & PEG-4000	6.22
PEG-4000	3.44×10^{-7}	—	—
PEG-1000	1.88×10^{-7}	—	—
PEG-600	1.44×10^{-7}	—	—
PEG-400	1.2×10^{-7}	—	—

To compare the theoretical predictions with experiment, it is necessary to plot the solubility of the protein in g/L vs. % PEG added (wt./vol.), where % PEG is defined as the grams of polymer added per 100 mL of the solution. The protein solubility and the concentration of PEG in % PEG units can be obtained from the volume fractions in a fairly straightforward manner. As defined earlier, $\phi_2 = (N_2\pi d_2^3)/(V_{tot}6)$ and $\phi_3 = (\pi n_3 d_3^3)/6 = (N_3\pi d_3^3)/[6V_{tot} - 6N_2(\pi d_2^3/6)]$. The number densities of the protein and polymer, ρ_2 and ρ_3, respectively, are thus given by $\rho_2 = 6\phi_2/\pi d_2^3$ and $\rho_3 = n_3(1 - \phi_2)$. Conversion of the number densities to mass units using molecular weights and Avogadro's number is all that is required to extract the conventional experimentally determined quantities, namely the solubility in g/L and % PEG in g/100 mL. Expressions for the solubility and % PEG are thus given by:

$$\log S(\text{g/L}) = \log\left[\frac{6{,}000\,\phi_2 M_2}{\pi d_2^3 N_{Av}}\right] \tag{10}$$

$$\%\text{PEG(g/100 mL)} = \frac{100\,M_3 n_3(1 - \phi_2)}{N_{Av}} \tag{11}$$

where ϕ_2 in Eq. 10 is the volume fraction of the protein in the liquid phase (at equilibrium with the solid or precipitate phase), and N_{Av} is the Avogadro number of molecules (used for conversion from molar to mass units).

Note that the above expressions for the solubility and % PEG contain a dependency on the molecular weights and the radii of the equivalent sphere of the protein and polymer. It is possible, however, to rewrite these expressions in terms of different macromolecular parameters that may be more accessible quantities from an experimental viewpoint. The volume of a hydrated sphere is given by Cantor and Schimmel (1980):

$$V_h = \frac{\pi d_2^3}{6} = \left(\frac{M_2}{N_{Av}}\right)(\overline{V}_2 + \delta_1 \overline{V}_1) \tag{12}$$

where $\overline{V}_2$ is the partial specific volume of the solute, $\overline{V}_1$ is the inverse specific density of water (solvent), and δ_1 is the hydration of the protein measured in g H_2O/g protein. Substitution of Eq. 12 into Eq. 10 results in an expression that depends only on the thermodynamic parameters defined above

$$\log S = \log\left[\frac{1{,}000\,\phi_2}{\overline{V}_2 + \delta_1 \overline{V}_1}\right] \tag{13}$$

An advantage of using this formalism over that of directly incorporating the radii is that there are predetermined ranges for the partial specific volumes and the hydration for globular proteins. Virtually all proteins have $\overline{V}_2$ values between 0.69 and 0.75 cm^3/g so long as they do not have extensive material other than amino acids in their composition (Cantor and Schimmel, 1980). Also, hydration values between 0.3 and 0.4 g H_2O/g protein are typical for globular proteins. It becomes a simple matter to generate solubility curves using typical values for these thermodynamic parameters once the diameter ratio of protein to polymer is known.

Comparison with experiment

Atha and Ingham investigated the precipitation of various proteins with added PEG. They used PEG of different molecular weights along with proteins of different sizes to determine the effect of size on solubility. Some of their results are summarized in Figures 1 and 2. Figure 1 shows the experimental solubility curves for different proteins upon the addition of PEG of molecular weight 4,000. Figure 2 illustrates the effect of PEG molecular weight on the solubility of one protein, human serum albumin (HSA).

Figures 6, 7 and 8 are the theoretical predictions for the systems described above, obtained using Eqs. 10 and 11 and the data in Table 1. In Figure 6, solubility curves are predicted for four proteins (Fibrinogen, Thyroglobulin, γ-globulin, and Aldolase). We note immediately that the linearity of the solubility curve does not extend to all PEG concentrations. This suggests that extrapolation of the linear part of the curve to zero PEG concentrations may not give a physically realistic "intrinsic" solubility. A comparison of Figures 1 and 6 shows reasonable qualitative agreement. The theoretical curves are in the same range as the experimental data. We note, however, that while our predictions strictly follow the general trend that larger proteins precipitate easier than smaller ones, ($d_{Fib} > d_{IgG} > d_{Thy} > d_{Ald}$) Thyroglobulin and Aldolase are reversed in the experimental data. One possible explanation is that the experiments were conducted at a pH of 7.0, which is closer to the isoelectric point of Aldolase than Thyroglobulin. (Recall that all proteins exhibit a minimum solubility at the isoelectric point.) The lack of quantitative agreement may also be due to the fact that the proteins, which were compared with our results, are far from globular, while the model is strictly valid only for spherical (more loosely, globular) proteins.

Figure 7 is a plot of the solubility of HSA for different

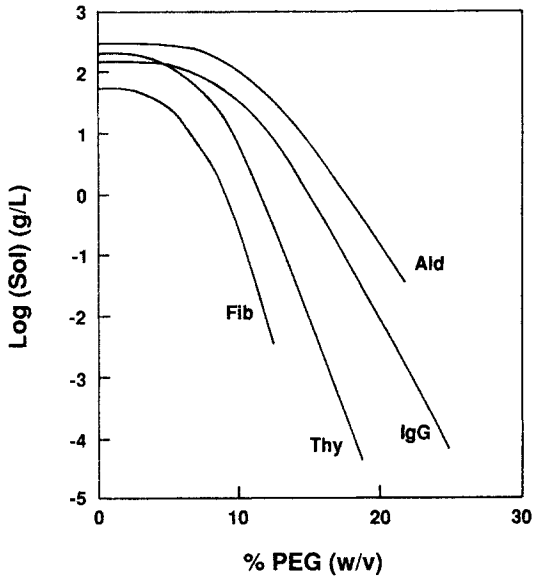

Figure 6. Theoretical predictions of the solubilities of four proteins with PEG-4000.

molecular weights of PEG. A comparison of Figures 2 and 7 reveals reasonable qualitative agreement, while there is only fair agreement on a quantitative basis. The observed experimental trend of increasing solubility with decreasing molecular weight of PEG is correctly predicted by the theory. Hence, the first three experimental trends observed in such systems and described earlier have been reproduced by the theory. At this point it is important to comment on the range of validity of the perturbation-theory approach.

As noted earlier, the volume-exclusion potential increases in depth while decreasing in range as the diameter ratio of protein to polymer is increased. The perturbation expansion used breaks down (fails to converge) for diameter ratios greater than 10 or less than 2.5. For the small diameter ratios, the potential becomes long-ranged, and the truncation of the perturbation at the second-order term is no longer adequate. For larger diameter ratios, the attractive well gets deeper, resembling the so-called "sticky sphere" state. (In both cases, the hard-sphere model is no longer adequate as a reference state and the perturbation terms increase in magnitude.) We therefore restrict ourselves to diameter ratios within this range. For this reason, in Figure 7 where the protein diameter is fixed (HSA) we are restricted to an upper limit of the PEG molecular weight of about 1,000.

We have performed calculations for diameter ratios other than those shown in Figure 7. Figure 8 illustrates the effect of polymer molecular weight on the solubility of thyroglobulin. (Only the linear portion of the curve is drawn.) The trend of increasing solubility with decreasing molecular weight of polymer is maintained. Note that, since thyroglobulin is a larger protein, we can predict solubility curves for higher molecular weights of PEG, while still confining oursevles to the range of diameter ratios described above. Recall that, other theories developed to explain the precipitation phenomenon have been unable to explain all of the experimental trends. For instance, Atha and Ingham (1981) predicted the opposite trend of the solubility with polymer molecular weight to that observed. They plotted the slopes of the solubility curves as a function of PEG molecular weight and found the behavior to be the opposite of the experimental observations.

In view of the fact that no adjustable parameters are included in the model, the qualitative agreement produced seems to suggest that our choice of the intermolecular potential is reasonable. Although the underlying mechanism behind PEG-induced precipitation, namely volume-exclusion, has been included and accounted for in the theory, there are other factors that play a role in determining the final composition. The model, as it stands, cannot predict solubility variations with pH or ionic strength. The parameters that warrant inclusion are mainly

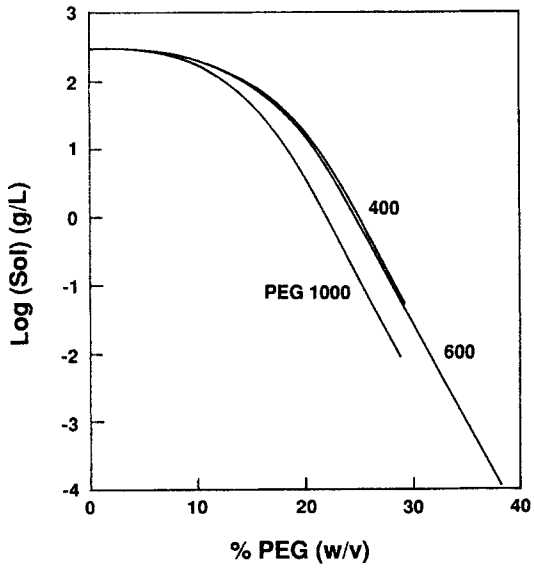

Figure 7. Theoretical predictions of the variation of the solubility of a single protein with molecular weight of PEG.

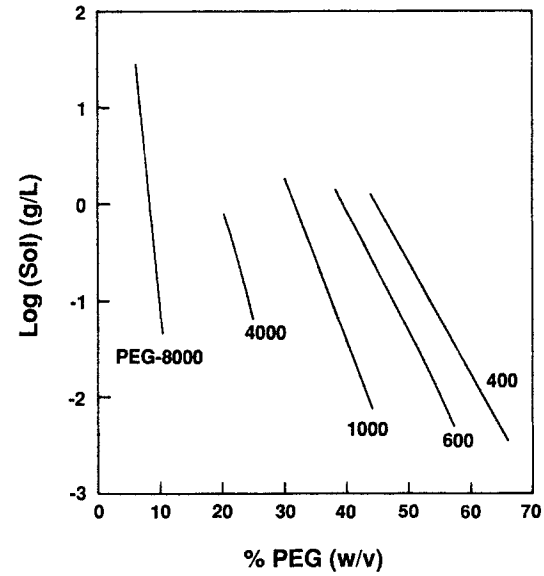

Figure 8. Theoretical predictions of the variation of the solubility of thyroglobulin with molecular weight of PEG.

electrostatic terms as evidenced by a dependence of the solubility curve on the pH as shown in Figure 9 (obtained from Atha and Ingham, 1981). Hence, it seems likely that an inclusion of electrostatic effects into the model should provide a more reliable predictive ability to the theory. This refinement to the intermolecular potential and the effect it has on the solubility curve is discussed in the next section.

Inclusion of Electrostatic Interactions

To explain the experimentally observed variations in the solubility with pH and ionic strength, forces other than those arising from volume-exclusion effects need to be included in the model. Here, we add an electrostatic interaction term to the intermolecular potential.

Intermolecular potential

The functional form for this potential depends on the size of the electrical double layer relative to the particle size (Verwey and Overbeek, 1948). For thin double layers, we use the interaction potential developed by Derjaguin (Derjaguin, 1934; Verwey and Overbeek, 1948) for charged spheres at infinite dilution in a dielectric medium.

$$u_R(r) = \frac{\epsilon d \psi_0^2}{4} \ln \{1 + \exp [-\kappa(r - d)]\} \tag{14}$$

where r is the distance between centers of spheres, ϵ is the dielectric constant of the solvent (fixed at 80), ψ_0 is the surface potential, κ is the inverse Debye length, and d is the sphere diameter. This form for the potential is valid for small Debye lengths relative to the particle radius ($d\kappa > 20$), with κ defined as follows

$$\kappa = \left\{\frac{8\pi e^2 N_{Av} I}{1{,}000\,\epsilon k T}\right\}^{1/2} \tag{15}$$

where e is the charge of an electron and I the ionic strength of the solution. We set T to 298 K in all our calculations. If $d\kappa$ is small ($d\kappa < 5$), the above form for the interaction potential is invalid, and we use the following expression from Verwey and Overbeek for the potential energy of interaction between two spherical double layers.

$$u_R(r) = \frac{\epsilon d^2 \psi_0^2}{4} \frac{\exp [-\kappa(r - d)]}{r} \beta \tag{16}$$

in which

$$\beta = \frac{1 + \alpha}{1 + \dfrac{e^{-\kappa(r-d)}}{2 r d\kappa}(1 + e^{-d\kappa})(1 + \alpha)} \tag{17}$$

The parameters α in Eq. 17 is in turn calculated from

$$\alpha = \lambda_1 \left(1 + \frac{1}{rd\kappa}\right) + \lambda_2 \left(1 + \frac{3}{rd\kappa} + \frac{3}{(rd\kappa)^2}\right) \tag{18}$$

where λ_1 and λ_2 are obtained by solving the following two equations simultaneously.

$$\begin{aligned} 0 = \frac{\lambda_1}{3} + \frac{e^{-\kappa(r-d)}}{2 r d\kappa} \left\{\frac{\frac{d\kappa}{2} - 1}{\frac{d\kappa}{2} + 1} + e^{-d\kappa}\right\} \left\{\left(1 + \frac{1}{rd\kappa}\right)\right. \\ + \lambda_1 \left[1 + \frac{2}{rd\kappa} + \frac{2}{(rd\kappa)^2}\right] \\ \left. + \lambda_2 \left[1 + \frac{4}{rd\kappa} + \frac{9}{(rd\kappa)^2} + \frac{9}{(rd\kappa)^3}\right]\right\} \end{aligned} \tag{19}$$

$$\begin{aligned} 0 = \frac{\lambda_2}{5} + \frac{e^{-\kappa(r-d)}}{2 r d\kappa} \left\{\frac{d\kappa^2 - 3d\kappa + 3}{d\kappa^2 + 3d\kappa + 3} - e^{-d\kappa}\right\} \left\{\left(1 + \frac{3}{rd\kappa} + \frac{3}{rd\kappa^2}\right)\right. \\ + \lambda_1 \left[1 + \frac{4}{rd\kappa} + \frac{9}{(rd\kappa)^2} + \frac{9}{(rd\kappa)^3}\right] \\ \left. + \lambda_2 \left[1 + \frac{6}{rd\kappa} + \frac{24}{(rd\kappa)^2} + \frac{54}{(rd\kappa)^3} + \frac{54}{(rd\kappa)^4}\right]\right\} \end{aligned}$$

Hence, depending on the value of $d\kappa$, either Eq. 14 or 16 can be used to calculate the electrostatic repulsion. An analysis of the variation of both forms of the potential with distance and $d\kappa$ helps decide where the crossover from Eq. 14 to 16 should occur (see figure in Verwey and Overbeek, 1948). We use Eq. 16 for values of $d\kappa$ lower than 5.0 and Eq. 14 for $d\kappa > 20.0$. In the intermediate region, the equation yielding the lower value for the repulsion is used, as both Eqs. 14 and 16 are known to overpredict the repulsive potential. This potential is added on to the volume-exclusion potential of Eq. 1. We note that Gast et al. have also considered electrostatic interactions in their paper.

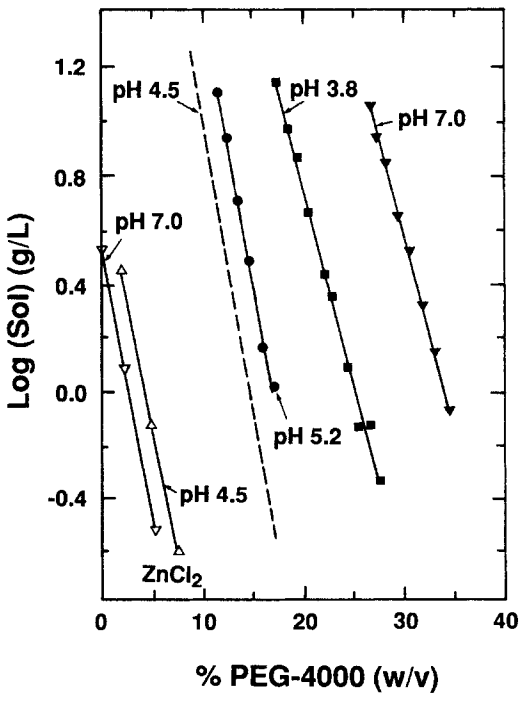

Figure 9. Variation of the solubility of proteins with pH.
From D. H. Atha and K. C. Ingham, *J. Bio. Chem.*, **256**, 12108 (1981). See reference for details of solution conditions.

However, they used only the infinite dilution potential (flat surface approximation, valid for large $d\kappa$'s) to represent the repulsion since this is appropriate to the colloid-polymer problem. Their final potential after addition of electrostatic terms exhibits a steep repulsion due to the high value of the prefactor $(\epsilon d\psi_0^2)/4$.

The model developed previously can now account for pH and ionic strength variations as described subsequently. The electrostatic interaction is a function of the Debye length κ and the surface potential ψ_0. It remains to relate these quantities to the pH and the ionic strength. The ionic strength enters the intermolecular potential directly via the Debye length, with $\kappa \approx 3.28 \times 10^7 (I)^{0.5}\ \text{cm}^{-1}$. Variations in the pH are accounted for in a more indirect way. From the Guoy-Chapman treatment of the double layer, where the limitations of the Debye-Hückel theory are removed (Hiemenz, 1977), one can relate the surface potential ψ_o to the surface charge density σ as,

$$\psi_0 = \frac{2kT}{ze} \sinh^{-1}\left(\frac{2\pi ze\sigma}{\epsilon kT\kappa}\right) \tag{20}$$

The variation of σ with pH is obtained from experimentally measured titration curves which plot the variation of the charges dissociated per molecule of a protein vs. pH. From a plot of this nature (Tanford et al., 1955), which gives the total number of surface charges at a fixed pH, we calculate the surface charge density for our spherical molecule and obtain the surface potential from Eq. 20. Hence, by altering ψ_0 in the intermolecular potential, we can model pH variation in experimental systems.

The variations of the attractive (excluded volume), repulsive (electrostatic) and the total potential with distance for four cases of interest in this study are shown in Figures 10a and 10b. Figure 10a is for a diameter ratio of $d_2/d_3 = 2.7$, $\phi_3 = 0.40$ and charges dissociated per protein of ten. The only parameter varied is the ionic strength ($I = 0.20, 0.30$). Figure 10b is drawn for a different diameter ratio (5.86); but is identical to Figure 10a in all other respects. A comparison of Figures 10a and 10b with the purely attractive volume-exclusion potential reveals that the addition of the electrostatic interaction term does not drastically alter the characteristics of the original intermolecular potential. This is important because it is the volume-exclusion mechanism that is responsible primarily for the phase transition and any refinements made should not completely change the overall character of the potential.

It is worthwhile to examine the behavior of the overall potential for various values of the parameters. From Figures 10a and 10b we note that, obviously, the attractive portion of the curve is unaffected by ionic strength, while the repulsion (and therefore the overall potential) is diminished in range by an increase in ionic strength. The magnitude of the repulsion depends essentially on the surface potential ψ_0. In cases of interest in these studies, the volume-exclusion attraction is dominant at small separations, but the range of the overall potential is greater than that of the pure attraction. The potential has the characteristics of a mermaid potential (attractive head and a repulsive tail) as can be seen in the figures. As mentioned earlier, this contrasts with the Gast et al. (1983) potential, which exhibits a steep repulsion at short separations.

Since the overall potential does not show a steep repulsion at short separations we can use the same type of perturbation theory discussed earlier. It must be ensured, however, that the perturbation expansion is still valid for the new potential. This is done as before by checking that the second-order term in

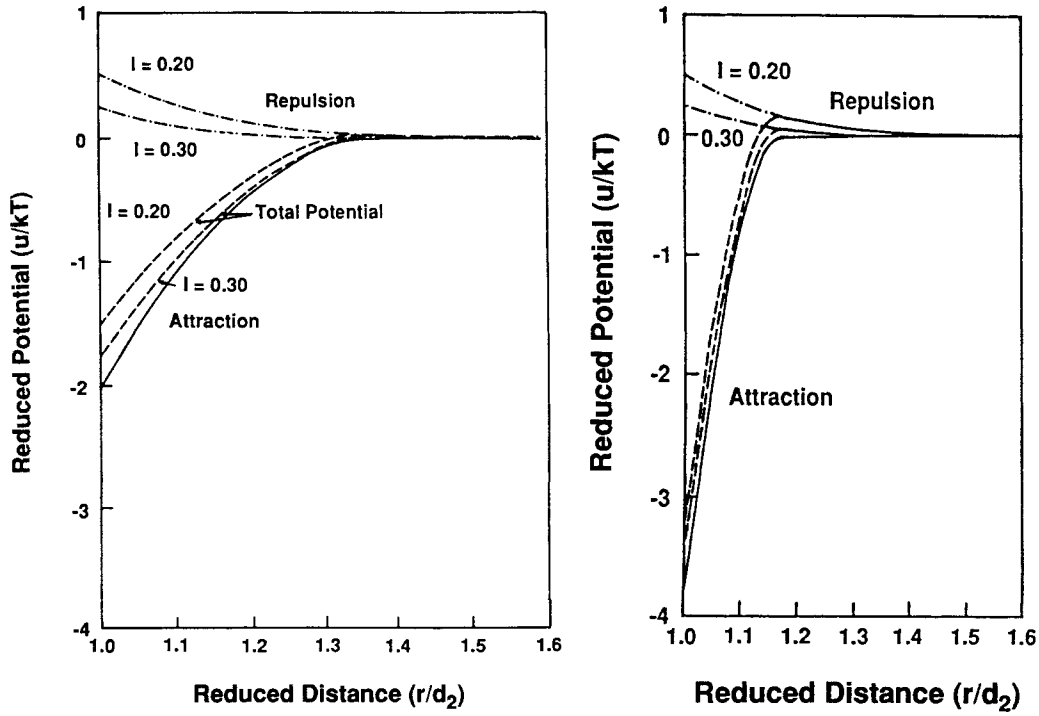

Figure 10. Variation of the reduced potential with reduced distance.

(a) $d_2/d_3 = 2.7$
(b) $d_2/d_3 = 5.86$

the expansion remains much smaller in magnitude than the first-order correction.

Solubility Calculations

The overall potential (the sum of Eq. 1 and Eq. 14 or 16) is used to calculate the Helmholtz free energy via Eq. 3. The Gibbs free energy and the pressure are calculated as before from Eqs. 4 and 5. The solubility calculations are performed for representative values of bovine serum albumin to polymer (BSA-PEG) diameter ratios, and for various pH values obtained from Tanford et al. (1955). Ionic strength values ranging from 0.05 to 0.30 are chosen consistent with typical experimental systems. Since the following discussion uses the titration data from Tanford et al. as a basis for the pH values, the solubility curves obtained are valid only for BSA-PEG mixtures of differing molecular weights. Solubility plots illustrating the variation of protein solubility with %PEG are obtained as described previously. Next, we offer a systematic analysis of the variation effects in each parameter on the solubility of the protein when all other parameters are held fixed.

First, the dependence of the solubility on the ionic strength is investigated. In Figure 11, the diameter ratio and the pH are held constant at 2.7 and 4.2, respectively, and four ionic strength values are considered. [This pH value is also equivalent to a pH of 8.8 (Tanford et al., 1955).] As the ionic strength of the solution is increased for the same protein-polymer pair at constant pH, the solubility decreases. This is an expected result; as ionic strength is increased, the electrostatic repulsions are screened out and the protein behaves increasingly like an uncharged molecule. A closer examination of this plot shows that with increasing ionic strength the solubility curves approach the results explained previously. This is the pure volume-exclusion result (no electrostatic interaction) and is shown as the dashed line. We have also performed calculations for different values of the pH and the diameter ratio and the same trend is observed.

Second, we examine the effect of pH variation on the solubility at constant ionic strength and diameter ratio, as shown in Figure 12. In this figure three pH values are investigated (7.1, 8.8, and 10.7) at a fixed ionic strength of 0.10 and a diameter ratio of 5.86. As we move away from the isoelectric point (5.5 for BSA), more PEG needs to be added to precipitate the protein. This is exactly what is expected; all proteins exhibit the minimum solubility at the isoelectric point. Solubility curves studying the pH effects have also been generated for different values of the ionic strength and diameter ratio. In these cases too, an identical trend is observed.

Finally, we can study the effect of the diameter ratio on the solubility. We have already studied this effect but it is worthwhile to confirm that the predictions made earlier in this regard remain valid even after addition of the electrostatic interaction. Figure 13 shows the variation in the solubility of the protein with the diameter ratio at constant pH and ionic strength. Three different diameter ratios (2.7, 3.75, and 5.86) are considered. The prediction of a reduction in solubility with decreasing diameter ratio of protein-to-polymer remains unchanged.

To obtain solubilities of proteins using this method, one needs only a titration curve relating the surface charge to the pH, and an estimate of the diameter ratio between protein and polymer. If the size of the protein is unknown, alternate expressions for the solubility in terms of its partial specific volume and hydration can be used. It is also possible to use a knowledge of the three-dimensional structure of the protein to calculate the surface charge density (and hence ψ_0) as a function of pH, if titration curves are not available for the protein of interest.

Atha and Ingham (1981) have measured the pH dependence of the solubility of HSA in PEG 4000. However, the diameter ratio for this protein-polymer set is below the range of validity of

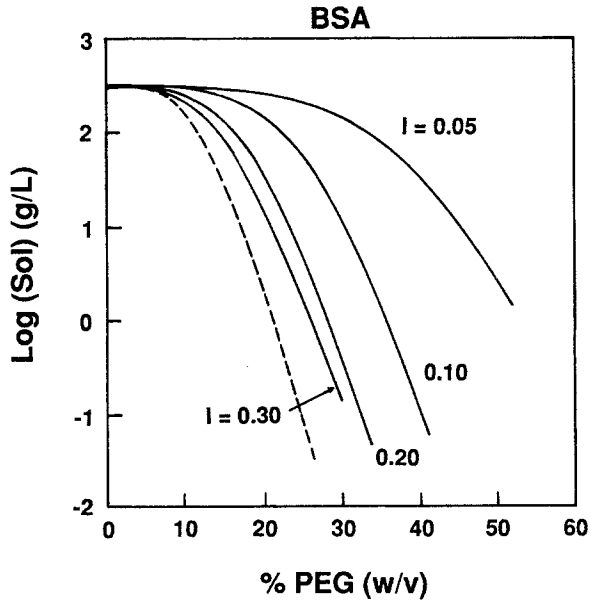

Figure 11. Theoretical predictions of the solubility variation of BSA with ionic strength at a fixed pH and PEG molecular weight.

$d_2/d_3 = 2.7$, pH = 4.2

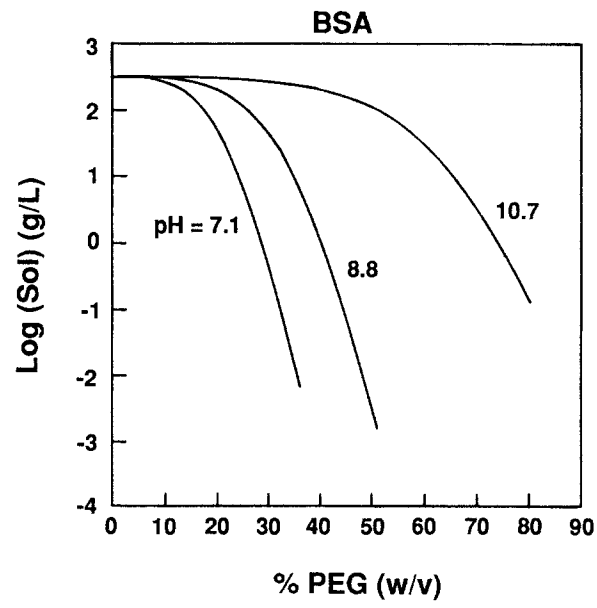

Figure 12. Theoretical predictions of the solubility variation of BSA with pH at a fixed ionic strength and PEG Molecular weight.

$d_2/d_3 = 5.86$, $I = 0.10$

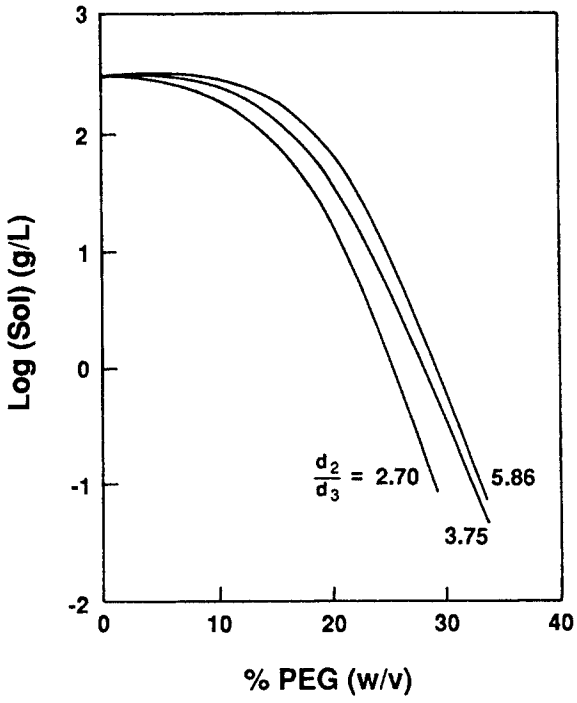

Figure 13. Theoretical predictions of the solubility variation of BSA with PEG molecular weight at a fixed pH and ionic strength.

the perturbation expansion. We are not aware of any other systematic experiments that have been performed to measure the effect of pH and ionic strength on the precipitation of proteins by nonionic polymer. Hence we are unable to make a quantitative comparison of these theoretical predictions of the variation in the solubility of proteins with electrostatic parameters with experimental results. We have used BSA as our sample protein because titration data relating the pH to σ were readily available. However, the conclusions made in regard to the solubility variations are applicable to all proteins.

Conclusion

A fairly simple fundamental theory has been outlined that can be used to predict protein solubilities in polymer solutions. The theory has been shown to correctly predict the trends in the variation of the solubility with all process parameters. Various approximations were made in the model including: the expressions for the intermolecular potentials, the assumption of pairwise additivity in the statistical mechanical analysis, and the inherent approximations of the Barker-Henderson perturbation expansion. We would like to reiterate that the model is, as yet, only qualitative and is not yet a tool to be used to obtain numbers for the solubility.

Acknowledgment

The authors gratefully acknowledge the support of the National Institutes of Health (Grant #1 RO 1-GM40023-02), the National Science Foundation (Grant #CBT-8720284), and the North Carolina Biotechnology Center.

Notation

A = Helmholtz free energy
D = diffusion coefficient
d = diameter of a molecule
e = charge of an electron
G = Gibbs free energy
$g(r)$ = radial distribution function
I = ionic strength of solution
k = Boltzmann's constant
M = molecular weight
N = number of molecules in system
N_{Av} = Avogadro's number of molecules
n_3 = number density of polymer molecules based on available volume
p = pressure
r = intermolecular distance
S = solubility of protein
T = absolute temperature
$U(r)$ = intermolecular pair potential
$\overline{V}_1$ = inverse specific density of solvent
$\overline{V}_2$ = partial specific volume of protein
V_{tot} = total volume of system
Z = thermodynamic compressibility

Greek letters

δ_1 = hydration of protein
ϵ = dielectric constant of solvent
κ = inverse Debye length
λ = perturbing parameter
η = viscosity
ϕ_0 = close-packed volume fraction, $(\pi/6)\sqrt{2} = 0.74$
ϕ = volume fraction of molecules
ρ = number density
ψ_0 = surface potential of protein

Subscripts

1 = solvent
2 = protein
3 = polymer
hs = hard sphere

Proteins and polymer

BSA = bovine serum albumin
HSA = human serum albumin
THY = thyroglobulin
IgG = γ-globin
ALD = aldolase
FIB = fibrinogen
PEG = polyethylene glycol

Literature Cited

Alder, B. J., W. G. Hoover, and D. A. Young, "Studies in Molecular Dynamics: V. High-Density Equation of State and Entropy for Hard Disks and Spheres," *J. Chem. Phys.*, **49**, 3688 (1971).

Arakawa, T., and S. N. Timasheff, "Mechanism of Poly(ethylene glycol) Interaction with Proteins," *Biochemistry*, **24**, 6756 (1985).

———, "Theory of Protein Solubility," *Methods in Enzymology*, **114**, 49 (1985).

Asakura, S., and F. Oosawa, "Interaction between Particles Suspended in Solutions of Macromolecules," *J. Polym. Sci.*, **33**, 183 (1958).

Atha, D. H., and K. C. Ingham, "Mechanism of Precipitation of Proteins by Polyethylene Glycols," *J. Biol. Chem.*, **256**, 12108 (1981).

Barker, J. A., and D. Henderson, "Perturbation Theory and Equation of State for Fluids: I. the Square-Well Potential," *J. Chem. Phys.*, **47**, 2856 (1967).

———, "Perturbation Theory and Equation of State for Fluids: II. a Successful Theory of Liquids," *J. Chem. Phys.*, **47**, 4714 (1967).

Bell, D. J., M. Hoare, and P. Dunnill, "The Formation of Protein Precipitates and their Centrifugal Recovery," *Adv. in Biochem. Engr./Biotechnol.* **26**, A. Fietcher, ed., Springer Verlag (1983).

Bjurstrom, E., "Biotechnology. Fermentation and Downstream Processing," *Chem. Eng.*, **92**, 151 (Feb. 18, 1985).

Cantor, C. R., and P. R. Schimmel, *Biophysical Chemistry*, Part 2, W. H. Freeman and Co. (1980).
Carnahan, N., and K. Starling, "Thermodynamic Properties of a Rigid-Sphere Fluid," *J. Chem. Phys.*, **53**, 600 (1970).
Caughlin, T. R., and A. R. Thomson, *Proteins, Recovery and Purification*, Harwell, Oxfordshire, U.K. (Nov., 1983).
Chun, P. W., M. Fried, and E. F. Elliot, "Use of Water-Soluble Polymers for the Isolation and Purification of Human Immunoglobulins," *Anal. Biochem.*, **19**, 481 (1967).
De Hek, H., and A. Vrij, "Interactions in Mixtures of Colloidal Silica Spheres and Polystyrene Molecules in Cyclohexane," *J. Coll. Interf. Sci.*, **84**, 409 (1981).
Derjaguin, B., "Untersuchungen uber die Reibung und Adhasion: IV," *Kolloid-Z.*, **69**, 155 (1934).
Dickman, R. personal communication (1988).
Edmond, E., and A. G. Ogston, "An Approach to the Study of Phase Separation in Ternary Aqueous Systems," *Biochem. J.*, **109**, 569 (1968).
Faith, W. T., C. F. Neubeck, and E. T. Reese, "Advances in Biochemical Engineering: I," Ghose T. K. and Fietcher A. (eds.), Springer Verlag, New York (1971).
Foster, P. R., P. Dunnill, and M. D. Lilly, "The Precipitation of Enzymes from Cell Extracts of Saccharomyces Cerevisiae by Polyethylene Glycol," *Biochem. Biophys. Acta*, **317**, 505 (1973).
Gast, A. P., C. K. Hall, and W. G. Russell, "Polymer-Induced Phase Separations in Nonaqueous Colloidal Suspensions," *J. Coll. Interf. Sci.*, **96**, 251 (1983).
Gast, A. P., C. K. Hall, and W. G. Russell, "Phase Separations Induced in Aqueous Colloidal Suspensions by Dissolved Polymer," *Farad. Discuss. Chem. Soc.*, **76**, 189 (1983).
Haire, R. N., W. A. Tisel, J. G. White, and A. Rosenberg, "On the Precipation of Proteins by Polymers: The Hemoglobin-Polyethylene Glycol System," *Biopolymers*, **23**, 2761 (1984).
Hall, K. R., "Another Hard-Sphere Equation of State," *J. Chem. Phys.*, **57**, 2252 (1971).
Hasko, F., R. Vaszileva, and L. Halaz, "Solubility of Plasma Proteins in the Presence of Polyethylene Glycol," *Biotechnol. & Bioeng.*, **24**, 1931 (1982).
Hiemenz, P. C., *Principles of Colloid and Surface Chemistry*, Marcel Dekker, New York (1977).
Hönig, W., and M. R. Kula, "Selectivity of Protein Precipitation with PEG fractions of various Molecular Weights," *Anal. Biochem.*, **72**, 502 (1976).
Ingham, K. C., "Polyethylene Glycol in Aqueous Solution: Solvent Perturbation and Gel Filtration Studies," *Arch. Biochem. Biophys.*, **184**, 59 (1977); "Precipitation of Protein with PEG: Characterization of Albumin," *ibid.*, **186**, 106 (1978).
Iverius, P. H., and T. C. Laurent, *Biochem. Biophys. Acta.*, **133**, 371 (1967).
Kincaid, J. M., and J. J. Weis, "Radial Distribution Function of a Hard-Sphere Solid," *Molec. Phys.*, **34**, 931 (1977).
Knoll, D., and J. Hermans, "Polymer-Protein Interactions," *J. Biol. Chem.*, **258**, 5710 (1983).
Kula, M. R., W. Hönig, and H. Foellmer, "Proceedings of the International Workshop on Technology for Protein Separation and Improvement of Blood Plasma Fractionation," H. E. Sandberg, ed., National Institutes of Health, Bethesda, MD (1978).
Laurent, T. C., "The Interaction between Polysaccharides and other Macromolecules: V. The Solubility of Protein in the Presence of Dextran," *Biochem. J.*, **89**: 253 (1963).
Lee, L. L. Y., and J. C. Lee, "Thermal Stability of Proteins in the Presence of Polyethylene Glycols," *Biochemistry*, **26**, 7813 (1987).
McQuarrie, D. L., *Statistical Mechanics*, Harper and Row, New York (1976).
Middaugh, C. R., W. A. Tisel, R. N. Haire, and A. Rosenberg, "Determination of the Apparent Thermodynamic Activities of Saturated Protein Solutions," *J. Biol. Chem.*, **254**, 367 (1979).
Miekka, S. I., and K. C. Ingham,, "Influence of Self Association of Proteins on their precipitation by Poly(ethylene Glycols)," *Arch. Biochem. Biophys.*, **191**, 525 (1978).
Ogston, A. G., and C. F. Phelps, "The Partition of Solutes between Buffer Solutions and Solutions Containing Hyaluronic Acid," *Biochem. J.*, **78**, 827 (1961).
———, "Some Thermodynamic Relationships in Ternary Systems, with Special reference to the Properties of Systems Containing Hyaluronic Acid," *Arch. Biochem. Biophys. Suppl.*, **1**, 39 (1962).
Polson, A., G. M. Potgeiter, J. F. Largier, G. E. F. Mears, and F. H. J. Joubert, "The Fractionation of Protein Mixtures by Linear Polymers of High Molecular Weight," *Biochem. Biophys. Acta*, **82**, 463 (1964).
Scopes, R., "Protein Purification," Springer Verlag, New York (1982).
Smith, W. R., and D. Henderson, "Analytical representation of the Percus-Yevick hard-sphere radial distribution function," *Molec. Phys.*, **19**, 411 (1970).
Tanford, C., S. A. Swanson, and W. S. Shore, "Hydrogen Ion Equilibria of Bovine Serum Albumin," *J. Amer. Chem. Soc.*, **77**, 6414 (1955).
Verlet, L., and J. J. Weis, "Equilibrium Theory of Simple Liquids," *J. Phys. Rev. A*, **5**, 939 (1972).
Verwey, E. J. W., and J. T. G. Overbeek, *Theory of the Stability of Lyophobic Colloids*, Elsevier, New York (1948).
Zeppezauer, M., and S. Brishammar, "Protein Precipitation by Uncharged Water-Soluble Polymers," *Biochim. Biophys. Acta*, **94**, 581 (1965).

Manuscript received Apr. 3, 1990, and revision received Aug. 6, 1990.